Vol 14 No 12, December 2005
1009-1963/2005/14(12)/2491-05

Chinese Physics

© 2005 Chin. Phys. Soc.
and IOP Publishing Ltd

Improvement in refractive-index change in $LiNbO_3$:Ce:Cu by applying an external electric field*

Dai Cui-Xia(戴翠霞), Liu Li-Ren (刘立人)†, Liu De-An (刘德安),
Zhou Yu(周 煜), Chai Zhi-Fang(柴志方), and Luan Zhu(栾 竹)

Shanghai Institute of Optics and Fine Mechanics, Chinese Academy of Sciences, Shanghai 201800, China

(Received 3 February 2005; revised manuscript received 29 September 2005)

By jointly solving two-centre material equations with a nonzero external electric field and coupled-wave equations, we have numerically studied the dependence of the non-volatile holographic recording in $LiNbO_3$:Ce:Cu crystals on the external electric field. The dominative photovoltaic effect of the non-volatile holographic recording in doubly doped $LiNbO_3$ crystals is directly verified. And an external electric field that is applied in the positive direction along the c-axis (or a large one in the negative direction of the c-axis) in the recording phase and another one that is applied in the negative direction of the c-axis in the fixing phase are both proved to benefit strong photorefractive performances. Experimental verifications are given with a small electric field applied externally.

Keywords: non-volatile holographic recording, external electric field, refractive-index change, $LiNbO_3$:Ce:Cu crystals
PACC: 4240E, 7820W, 4280T, 4265

1. Introduction

Non-volatile holographic recording in $LiNbO_3$ (LN):Fe:Mn crystals has become an interesting topic since it was proposed[1] in hopes of solving the problem of washing out the stored information in singly doped LN crystals in the readout stage. The characteristics of LN:Fe:Mn crystals have ever since been investigated extensively,[2−4] and the application of such a crystal to holographic memory has been reported.[5,6] Recently, LN:Ce:Cu crystal is found to be another promising photorefractive material for non-volatile holographic recording and it attracts much attention of all because it can provide a high and persistent refractive-index change with weak light-induced scattering.[7−9] For optimizing the holographic recording in this promising photorefractive material, theoretical analyses of the dopant densities and the oxidation–reduction processing for LN:Fe:Mn crystals are extensively made.[10−16]

However, in all extensive investigations of optimizations of LN:Ce:Cu crystals, the low photon excitation efficiency (only about one out of one hundred absorbed photons can excite an electron) restricts the practical optimization capacity, and the depth of the total grating is greatly reduced as a result of a phase difference of 180 degrees between shallow and deep gratings.[1,12] So, the insufficient value of refractive-index change (RIC) requires an additional energy added to the crystal. In this paper, it is suggested that an external electric field (EEF) is used to provide the additional drift energy for LN:Ce:Cu crystals, which was proved to be able to improve the holographic recording in singly doped LN crystals.[17,18] Different from its application only to holographic recording in singly doped LN crystals, the EEF can be applied not only to the recording but also to the fixing phases of non-volatile holographic recording. Due to the dominative photovoltaic effect in doubly doped LN crystals, which is clearly proved by the spatial phase shift (SPS) between the grating and the light interference pattern, remarkable improvement in RIC is obtained

*Project supported by the State Science and Technology Commission of China (Grant No 2002CCA03500) and the National Natural Science Foundation of China (Grant No 60177016).
†E-mail: lirenliu@mail.shcnc.ac.cn

by applying an EEF in the positive direction along the c-axis (or a large EEF in the negative direction of the c-axis) in the recording, and by applying an EEF in the negative direction of the c-axis in the fixing phase.

2. The unified theory for the electric-field-related photorefractive process

2.1. Material equations with nonzero EEF

In general, the two-centre holographic recording can be described by Kukhtarev equations modified for doubly doped crystals.[12,13] When two ordinary-polarized, coherent writing beams are symmetrically incident upon the crystal and propagate in the xz plane, a sinusoidal interference pattern along the x-axis (c-axis) is produced, along which an EEF is applied. As usual, each variable is assumed to vary sinusoidally with x, and is replaced by its average and fundamental component of the Fourier series (denoted by the subscripts of 0 and 1). Then, the two-centre material equations with a nonzero EEF can be separated into two sets of zeroth- and first-order equations as follows:

$$\frac{\partial N_{\mathrm{D0}}^{-}}{\partial t} = -g_{\mathrm{D}} N_{\mathrm{D0}}^{-} + \gamma_{\mathrm{D}} N_{\mathrm{e0}}(N_{\mathrm{D}} - N_{\mathrm{D0}}^{-}), \tag{1}$$

$$\frac{\partial N_{\mathrm{S0}}^{-}}{\partial t} = -g_{\mathrm{S}} N_{\mathrm{S0}}^{-} + \gamma_{\mathrm{S}} N_{\mathrm{e0}}(N_{\mathrm{S}} - N_{\mathrm{S0}}^{-}), \tag{2}$$

$$N_{\mathrm{e0}} = \frac{g_{\mathrm{D}} N_{\mathrm{D0}}^{-} + g_{\mathrm{S}} N_{\mathrm{S0}}^{-}}{\gamma_{\mathrm{D}}(N_{\mathrm{D}} - N_{\mathrm{D0}}^{-}) + \gamma_{\mathrm{S}}(N_{\mathrm{S}} - N_{\mathrm{S0}}^{-})}, \tag{3}$$

and

$$\begin{aligned}\frac{\partial N_{\mathrm{D1}}^{-}}{\partial t} =& -g_{\mathrm{D}} N_{\mathrm{D1}}^{-} - S_{\mathrm{D,L}} m I_{\mathrm{L0}} N_{\mathrm{D0}}^{-} \\ &+ \gamma_{\mathrm{D}} N_{\mathrm{e1}}(N_{\mathrm{D}} - N_{\mathrm{D0}}^{-}) - \gamma_{\mathrm{D}} N_{\mathrm{e0}} N_{\mathrm{D1}}^{-},\end{aligned} \tag{4}$$

$$\begin{aligned}\frac{\partial N_{\mathrm{S1}}^{-}}{\partial t} =& -g_{\mathrm{S}} N_{\mathrm{S1}}^{-} - S_{\mathrm{S,L}} m I_{\mathrm{L0}} N_{\mathrm{S0}}^{-} \\ &+ \gamma_{\mathrm{S}} N_{\mathrm{e1}}(N_{\mathrm{S}} - N_{\mathrm{S0}}^{-}) - \gamma_{\mathrm{S}} N_{\mathrm{e0}} N_{\mathrm{S1}}^{-},\end{aligned} \tag{5}$$

$$N_{\mathrm{e1}} = \frac{\left\{\begin{array}{l}(g_{\mathrm{D}} + \gamma_{\mathrm{D}} N_{\mathrm{e0}}) N_{\mathrm{D1}}^{-} + (g_{\mathrm{S}} + \gamma_{\mathrm{S}} N_{\mathrm{e0}}) N_{\mathrm{S1}}^{-} - \dfrac{e\mu N_{\mathrm{e0}}}{\varepsilon\varepsilon_0}(N_{\mathrm{D1}}^{-} + N_{\mathrm{S1}}^{-}) - \dfrac{\mathrm{i}K}{e}[\kappa_{\mathrm{D}} N_{\mathrm{D1}}^{-} \\ +\kappa_{\mathrm{S}} N_{\mathrm{S1}}^{-} + (\kappa_{\mathrm{D,L}} N_{\mathrm{D0}}^{-} + \kappa_{\mathrm{S,L}} N_{\mathrm{S0}}^{-}) m I_{\mathrm{L0}}] + (S_{\mathrm{D,L}} N_{\mathrm{D0}}^{-} + S_{\mathrm{S,L}} N_{\mathrm{S0}}^{-}) m I_{\mathrm{L0}}\end{array}\right\}}{\gamma_{\mathrm{D}}(N_{\mathrm{D}} - N_{\mathrm{D0}}^{-}) + \gamma_{\mathrm{S}}(N_{\mathrm{S}} - N_{\mathrm{S0}}^{-}) + \dfrac{e\mu N_{\mathrm{e0}}}{\varepsilon\varepsilon_0} + \dfrac{k_{\mathrm{B}} T \mu K^2}{e} - \mathrm{i}K\mu E_0}, \tag{6}$$

where $g_{\mathrm{D}} = S_{\mathrm{D,L}} I_{\mathrm{L0}} + S_{\mathrm{D,H}} I_{\mathrm{H}}$, $g_{\mathrm{S}} = S_{\mathrm{S,L}} I_{\mathrm{L0}} + S_{\mathrm{S,H}} I_{\mathrm{H}}$, $\kappa_{\mathrm{D}} = \kappa_{\mathrm{D,L}} I_{\mathrm{L0}} + \kappa_{\mathrm{D,H}} I_{\mathrm{H}}$, and $\kappa_{\mathrm{S}} = \kappa_{\mathrm{S,L}} I_{\mathrm{L0}} + \kappa_{\mathrm{S,H}} I_{\mathrm{H}}$. In the above, the subscripts D and S indicate the deep and shallow centres, and L and H denote the lower (red) and higher frequency (UV) light, respectively; N, N^{-}, and N_{e} are densities of centre, the electron in a centre, and the conducting electron, respectively; γ, S, κ T, k_{B}, I and K are the recombination coefficient, the photo-excitation constant, the bulk photovoltaic coefficient, crystal temperature, Boltzmann constant, the intensity of light and the spatial frequency of interference pattern, respectively; ε_0, e, ε and μ are the permittivity in free space, the electron charge, the dielectric coefficient and the electron mobility in the conduction band, respectively; E_0 is the EEF; The total intensity of red light I_{L0} is defined as $I_{\mathrm{L0}} = A_1 A_1^{*} + A_2 A_2^{*}$, and the complex light modulation m can be described as $m = \dfrac{2A_1 A_2^{*}}{I_{\mathrm{L0}}}$, where A_1 and A_2 are the complex wave amplitudes of the two recording beams.

The space-charge field (SCF) E_{sc} can be expressed as

$$E_{\mathrm{sc}} = \frac{-\mathrm{i}e}{\varepsilon\varepsilon_0 K}(N_{\mathrm{D1}}^{-} + N_{\mathrm{S1}}^{-} + N_{\mathrm{e1}}). \tag{7}$$

And the RIC n_1 can be obtained from the SCF E_{SC} according to the linear electro-optic effect

$$n_1 \exp(\mathrm{i}\phi_{n_1}) = -\frac{n_{\mathrm{o}}^3 \gamma_{13} E_{\mathrm{sc}}}{2}, \tag{8}$$

where n_{o} is the average refractive index of LN crystal for ordinary-polarized recoding light, γ_{13} is the electro-optic coefficient and ϕ_{n_1} is the complex angle of n_1.

2.2. Coupled-wave equations

With a little modification to Kogelnik theory of the static volume grating, the coupled-wave equations of the two red beams in the dynamic volume grating of the photorefractive crystals[14,15] can be described as

$$\cos(\theta)\frac{\mathrm{d}A_1}{\mathrm{d}z} = -\frac{\mathrm{i}\pi n_1}{\lambda}\exp(\mathrm{i}\phi_{n_1})A_2 - \frac{\alpha}{2}A_1, \tag{9}$$

$$\cos(\theta)\frac{\mathrm{d}A_2}{\mathrm{d}z} = -\frac{\mathrm{i}\pi n_1}{\lambda}\exp(-\mathrm{i}\phi_{n_1})A_1 - \frac{\alpha}{2}A_2, \quad (10)$$

where λ, α and θ are the wavelength, the absorption coefficient and the incident angle of the red beam inside the crystal, respectively.

The SPS which is defined as the phase of the grating with respect to the light interference pattern can be expressed as

$$\phi = \phi_{n_1} - \phi_m, \quad (11)$$

where ϕ_{m} is the complex angle of the modulation coefficient m.

Considering the light absorption, the intensity of UV light is given by

$$I_{\mathrm{H}} = I_{\mathrm{H0}}\exp(-\alpha_{\mathrm{UV}}z), \quad (12)$$

where α_{UV} and I_{H0} are the absorption coefficient and the total intensity of UV light respectively, and z is the depth of the crystal.

3. Numerical calculations and discussion

In this section, we study dependences of RICs and SPSs on the EEF applied to a 2-mm-thick LN:Ce:Cu crystal. The concentrations of Ce and Cu are $1.6\times10^{25}\mathrm{m}^{-3}$ and $3.8\times10^{24}\mathrm{m}^{-3}$respectively and the initial total electron concentration amounts to 90% of the concentration of deep centre Cu. In the recording phase, the iso-intensity recording beams (633nm, the incident angle is 6.5° inside the crystal) and UV light (365nm) are assumed to illuminate the crystal for 150 min, and the recorded grating reaches saturation. Then one of the red beams is used to readout the recorded grating for 100 min, and the final grating arrives at a fixed state. For calculations, we divide the crystal into a large number of layers each with a sufficiently small thickness along the depth z, and the dynamic processes for recording and fixing a non-volatile hologram can be analysed by jointly solving the two-centre material and coupled-wave equations by use of the fourth-order Runge-Kutta method with respect to time t and depth z on the following conditions: for recording, I_{H0} =200W/m^2, I_{L0} =5000 W/m^2; for fixing, I_{H0}=0, I_{L0} =2500 W/m^2. In calculation, the parameters used here are ε=28, μ=7.4×10^{-5} m^2/Vs, ε_0=8.85×10^{-12}As/Vm, e=1.6×10^{-19}C, T = 293K, k_{B} = 1.38×10^{-23}J/K, γ_{13} = 1.09×10^{-11}m/V, α_{UV} = 3500m^{-1}, α=178m^{-1}, γ_{D} = 2.4 × 10^{-13}m^3/s, γ_{S} = 1.65 × 10^{-14}m^3/s, $S_{\mathrm{D,L}}$=0, $S_{\mathrm{D,H}}$=3.6×10^{-5}m^2/J, $S_{\mathrm{S,L}}$=3.3×10^{-6}m^2/J, $S_{\mathrm{S,H}}$=3.8×10^{-5}m^2/J, $\kappa_{\mathrm{D,L}}$=0, $\kappa_{\mathrm{D,H}}$ = −1.1 × 10^{-32}m^3/V, $\kappa_{\mathrm{S,L}}$ = −7 × 10^{-34}m^3/V, $\kappa_{\mathrm{S,H}}$ = −1.4 × 10^{-32}m^3/V, and n_{o}=2.286.[9]

3.1. EEF applied in the recording phase

In Fig.1(a) plotted are the variations of the SPSs in the recording phase with the depth z under different EEFs. We can see that the SPSs are all close to 0° or 180° in these situations, which indicates that either the photovoltaic effect or the drift effect, or both of them, dominate in the recording phase in the crystal. At a zero EEF, the nearly 0° SPS gives a direct verification of the dominant photovoltaic effect in the crystal without EEF. So, in the recording phase, either the large photovoltaic field or the EEF, or both of them, benefit strong gratings built in the LN:Ce:Cu crystal.

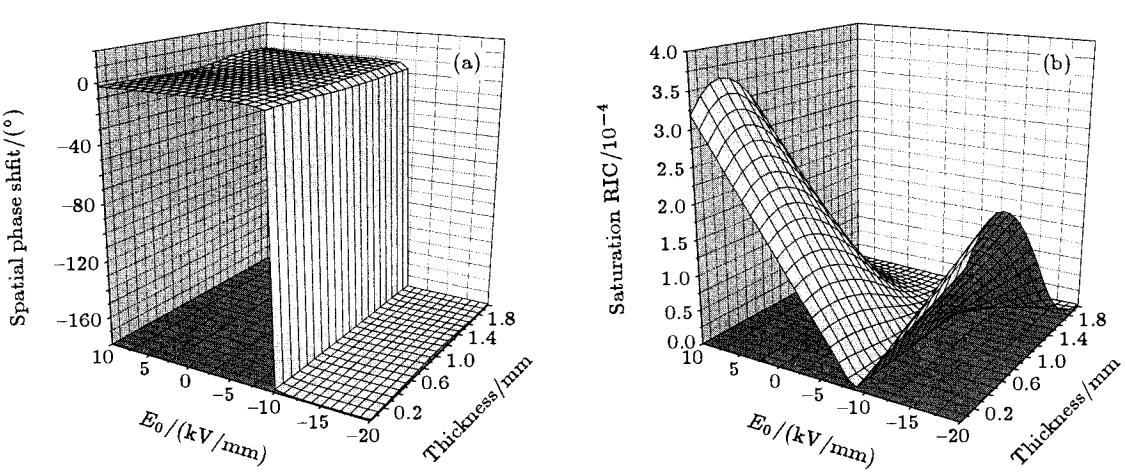


Fig.1. Variations of (a) SPSs and (b) saturation RICs with the depth of the crystal versus EEF E_0 applied in the recording phase. The mark "–" denotes the negative direction of the c-axis.

The variations of the saturation RICs with the depth z with different EEFs E_0 applied in the recording phase are presented in Fig.1(b). Due to the relatively strong absorption of UV-light, all the RICs undergo an increasing-to-maximum-to-decreasing process along the depth z. When an EEF is applied in the positive direction of the c-axis, the RICs increase with the increase of E_0; they drop down to a minimum when the EEF completely cancels the photovoltaic field, and grow afterward with the increase of EEF applied in the negative direction of the c-axis. The value of RIC can be greatly increased when E_0=10kV/mm is applied compared with that in the zero-field case. And the small value of the dominant diffusion electric field at the minimum location gives another verification of the dominative photovoltaic effect that the photovoltaic field is much greater than that of the diffusion in doubly doped LN crystals and the location of the minimum is a direct measure of the photovoltaic field in this system. Due to the dominative photovoltaic effect in this system, applying an EEF in the positive direction of the c-axis in the recording phase will add an additional drift field to the photovoltaic one and applying an EEF in the negative direction will cancel some portion or even total of it. So, stronger gratings will be recorded by applying an EEF along the positive direction of the c-axis or applying an EEF much larger than the photovoltaic field in the negative direction of the c-axis in the recording phase.

3.2. EEF applied in the fixing phase

As performed in the recording phase, we theoretically investigate the effect of EEF applied in the fixing phase on the fixed RICs when E_0=0 in the recording phase. In this section, the average fixed RICs are used to simulate their variations versus EEF.

Different from the mechanism in the recording phase, the mechanism in the fixing phase is much more complicated. Electrons are excited by reading red light from shallow ions and move in the conduction bands, and then they are finally trapped in a deep centre. Since there is a phase difference of nearly 180 degrees between the recorded shallow and deep gratings in the doubly doped LN crystal,[1,12] the large photovoltaic field and EEF in the positive direction of the c-axis in the fixing phase go against a strongly fixed grating. As shown in Fig.2, the fixed RICs increase with the increase of EEF applied in the negative direction of the c-axis, but in contrast they decrease with the EEF applied in the positive direction of the c-axis increasing. So, in the fixing phase of non-volatile holographic recording, an EEF in the negative direction of the c-axis should be applied in order to improve the photorefractive performance.

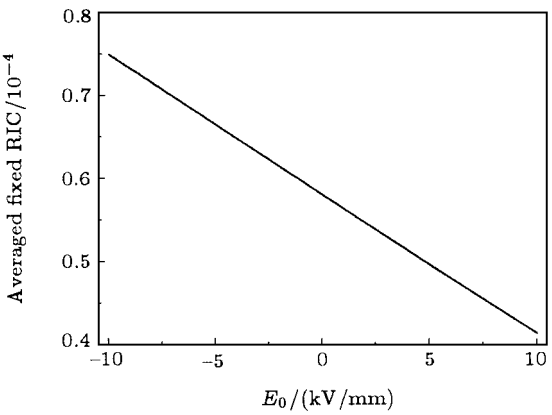


Fig.2. Variations of averaged fixed RICs versus EEF E_0 applied in the fixing phase. The mark "–" denotes the negative direction of the c-axis.

4. Experimental verification

4.1. Experimental setup and process

Experiments are performed with congruent 2-mm thick LN crystals doped with 0.307wt.% Ce_2O_3 and 0.011wt.% CuO, grown in air by the Czochralski method and annealed at 900° C in air for 6 hours. An ordinary-polarized beam from a 30-mW He–Ne laser is split into two beams each with an intensity of 2500W/m^2, which are incident upon the crystal symmetrically at an incident angle of 15°. The grating wave vector is aligned parallel to the c-axis of the crystal. The 365nm UV light for sensitization is produced with an intensity of 200W/m^2 from a 25-mW Ar^+ laser. In the experiments the crystals are pre-exposed to the UV for one hour. Then the holograms are recorded by the two interfering beams, together with the UV light, until quasi-saturation is reached. Finally, the holograms are fixed with only one He–Ne laser beam. In the experiments, the diffraction efficiency is defined as the ratio of the intensity of the diffracted light to that of the total reading light. During recording, one of the beams is blocked from time to time, and correspondingly another beam is diffracted from the recording grating, allowing us to evaluate the diffraction efficiency. During fixing, only the beam used for diffraction observation is still used for both readout and measurement.

4.2. Experimental results

Considering a practicable and inexpensive way to provide an EEF, we use a small field of 1kV/mm in this transmission geometry. The experimental results of applying the EEF in the recording phase are presented in Fig.3(a). Applying the EEF E_0=–1kV/mm can reduce the intensity of the photorefractive grating by cancelling a portion of the photovoltaic field, but applying the EEF E_0=1kV/mm will increase it by adding a drift field in the crystal. So, the diffraction efficiency is decreased when the EEF E_0=–1kV/mm is applied and enhanced when the EEF E_0=1kV/mm is applied.

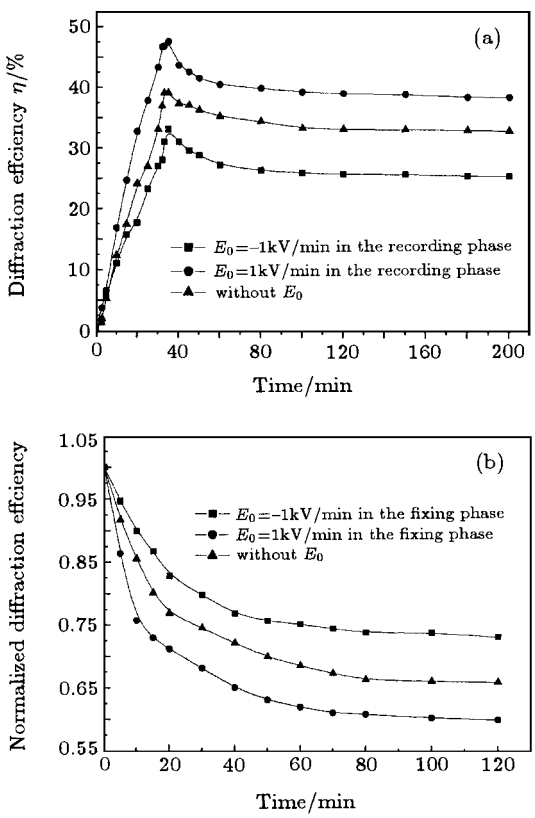


Fig.3. Variations of diffraction efficiency versus time under different EEFs separately applied in the recording phase (a) and in the fixing phase (b). The mark '–' denotes the negative direction of the c-axis.

The experimental results of applying an EEF in the fixing phase also show a well agreement with calculations which are plotted in Fig.3(b). Applying the EEF E_0=–1kV/mm will enhance the RIC, but applying the EEF E_0=1kV/mm will reduce the RIC in the crystal, so the final diffraction efficiency is increased by applying E_0=–1kV/mm and decreased by applying E_0=1kV/mm.

4.3. Discussion

Since the transmission geometry and the solid electrodes are adopted in experiments here in this article, a small EEF is used. In the reflection geometry, because the thickness of the crystal along the c-axis can be much smaller, a larger EEF may be easily applied by using liquid and transparent electrodes, thus a remarkable improvement will be observed. Here, active phase stabilization is ensured in this case where the fringe spacing of the holographic grating is much smaller than that in the transmission geometry.

5. Conclusion

On the basis of a unified theory for an electric-field-related photorefractive process, we investigate the dependences of the values of the RICs and SPSs on the EEF applied in the recording phase and also the dependences of the values of the averaged fixed RICs on the EEF applied in the fixing phase. Due to this two-centre system, RIC in the doubly doped LN:Ce:Cu crystals can be greatly improved by applying an EEF in the positive direction of the c-axis (or a large EEF in the opposite direction) in the recording phase and by applying an EEF in the negative direction of the c-axis in the fixing phase.

References

[1] Buse K, Adibi A and Psaltis D 1998 *Nature* **393** 665
[2] Adibi A, Buse K and Psaltis D 1999 *Appl. Phys. Lett.* **74** 3767
[3] Adibi A, Buse K and Psaltis D 2000 *Opt. Lett.* **25** 539
[4] Liu D, Liu L and Liu Y 2000 *Appl. Phys. Lett.* **77** 2964
[5] Adibi A, Buse K and Psaltis D 1999 *Opt. Lett.* **24** 652
[6] Adibi A, Buse K and Psaltis D 2001 *Appl. Opt.* **40** 5175
[7] Liu Y, Liu L and Zhou C 2000 *Opt. Lett.* **25** 908
[8] Liu Y, Liu L and Liu D 2001 *Opt. Commun.* **190** 339
[9] Ren L, Liu L and Liu D 2004 *Opt. Lett.* **29** 186
[10] Buse K 1997 *Appl. Phys.* B **64** 273
[11] Liu Y, Liu L and Zhou C 2000 *Opt. Lett* **25** 551
[12] Adibi A, Buse K and Psaltis D 2001 *J. Opt. Soc. Am.* B **18** 584
[13] Momtahan O and Adibi A 2003 *J. Opt. Soc. Am.* B **20** 449
[14] Ren L, Liu L and Liu D 2003 *J. Opt. Soc. Am.* B **20** 2162
[15] Kogelnik H 1969 *Bell Syst. Tech.* J **48** 2909
[16] Liu Y, Liu L, Zhou C and Xu L 2000 *Chin. Phys. Lett.* **17** 571
[17] Orlowskl R, Krätzig E and Kurz H 1977 *Opt. Commun.* **20** 171
[18] Luennemann Marc, Hartwig Ulrich and Buse Karsten 2003 *J. Opt. Soc. Am.* B **20** 1643